Development of a Simulation Tool for Field Cycled MRI

J. Alford[1], W. B. Handler[1], B. A. Chronik[1]

[1]Physics and Astronomy, University of Western Ontario, London, Ontario, Canada

Introduction: In field-cycled MRI [1], the homogeneous and static magnetic field produced by the superconducting magnet is replaced by two dynamically controlled magnetic fields. One field, the polarizing field, is responsible for magnetizing the sample. This field needs to be strong, but not particularly uniform or stable. The other field, the readout field, is required during the detection of the precessing magnetization. This field needs to be both stable and uniform, but not particularly strong. Contrast and SNR in field-cycled MR images are determined by a combination of the polarizing field waveform, the readout field waveform, the RF and gradient waveforms, and the sample characteristics. The particular complexities in predicting field-cycled image quality are: (1) the polarizing field is time dependent; (2) the readout field is time dependent; and (3) tissues have field-dependent T1 values.

In order to analyze the designs of proposed field-cycled MR systems, we have developed a comprehensive simulation tool that predicts image formation in a general case, using a classical picture of magnetization. Both the spatial and temporal dependencies of all fields (polarizing, readout, RF, and gradients) are combined with the spatial dependence of the sample and the T1 dispersion profiles of the tissues, to predict the formation of k-space and the subsequent processing to form the final image. Using this tool, we can predict the available contrast between various tissues as a function of the capabilities and operation of a proposed field-cycled system. We can also predict the effect of various degrees of system non-idealities on artefact production and SNR. We also expect to use the tool to assist in the debugging of an actual field-cycled system. The tool can also be used to predict image formation in a "normal" (non-field cycled) MRI system.

Methods: The equation describing the motion of magnetization, *M*, in a magnetic field is given by $M' = \gamma M \times B$ where γ is the gyromagnetic ratio. Within the rotating frame of reference the Cartesian components of magnetization are written as: $M_x' = -M_x/T2$, $M_y' = \gamma MzB1 - M_y/T2$, $M_z' = -\gamma MyB1 + (M_0 - M_z)/T1$ [2]. Here M_x, M_y and M_z are the components in the rotating frame, B1 is the RF strength, M_0, T1, T2 are functions of material and magnetic field strength and variation in the magnetic field from the average. It has been shown [3] that T1 in biological tissue can be approximated by equations of the form $T1 = \alpha v^{\beta}$ where ν is the product of $\gamma/2\pi$ and the applied field. T2 is not directly dependent on field strength and was treated as a constant of the tissue type, although the technique is capable of accommodating a field or time dependent T2.

A 4th order, adaptive Runge-Kutta method [4] was implemented to solve for *M* in a given field. Given a tissue matrix T(M0,T1,T2,x,y,z) and a matrix B(x,y,z,t) describing the magnetic field, the voxel magnetization matrix M(x,y,z,t) is solved within a user-specified error. For each coil, a three-dimensional magnetic field matrix was calculated at 100μm intervals for unit current using the Biot-Savart Law. Multiplying this three dimensional matrix by the corresponding one-dimensional timing waveform produced B(x,y,z,t), the four-dimensional matrix describing in space/time the resulting magnetic field. The total system magnetization in the lab frame at time, *t*, is a single vector given by $M_{system}(t) \propto \sum_{x,y,z}\left[\sum_{j}^{\text{all coils}} M_j(x,y,z,t)\right] \times \left[\hat{z}\gamma \int_0^t B(x,y,z,\tau)d\tau\right]$. A single column of *k-space* is produced by calculation of the magnetization at *n* evenly spaced intervals during the second half of the Y-gradient pulse.. A complete two-dimensional k-space map is built up by repeating the magnetization calculation for the entire range of X-gradient values. Finally the k-space is transformed into an image (see Figure1 (b) and (c)) via a fast-Fourier transform. The entire simulation requires ~90 minutes on a 1.2 GHz computer to generate a 96x96 pixel image.

Discussion: This software tool was coded in C++ to provide maximum flexibility of MRI system architecture, pulse sequence technique and computational platform. The flexibility of the timing waveform allows for any pulse sequence, noise amplitude or frequency, power supply fluctuation and electromagnetic interference. The library of tissues currently holds 18 different tissue types. The tissue library can be combined with tissue files creating virtual phantoms. Currently we have three virtual phantoms (3D): rat, monkey and human. As an example of the capability of the simulation, a timing waveform was optimized to produce maximum contrast between heart and liver with a field-cycled MRI system (Figure1 (b)) using the rat phantom (Figure 1 (a). The same image was generated for a non-field-cycled superconducting system of similar strength. Comparison of (b) and (c) indicates that additional contrast may be obtained by tailoring the field cycled MR timing waveforms to maximize the difference in magnetization between two tissues of similar proton density.

Figure 1. (a) Virtual phantom called the Visible Rat obtained from USAF. Cross-section through the thorax shows the heart, lungs and liver.

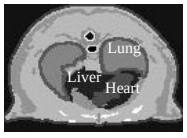

Figure 1. (b) Simulated superconducting MRI image showing proton density contrast between heart and liver tissue.

Figure 1. (c) Simulated field-cycled MRI image showing increased contrast between heart and liver tissue.

[1] Macovski et al., Magn Reson Med 30, 221-230 (1993)
[2] Cowan, Nuclear Magnetic Resonance and Relaxation, Cambridge 1997
[3] P.A. Bottomley, et al, Med. Phys. 11 (4), Jul/Aug 1984
[4] Numerical Recipes in C++, Cambridge University Press

Figure2. Timing waveforms for the polarizing (0.5 T), readout (5 MHz), and gradient fields for increased heart-liver contrast. The final waveforms show the magnetization of heart (lower, black) and liver (upper, gray) when subjected to these fields.